

Effects of Methanol on the Thermodynamics of Iron(III) [Tetrakis(pentafluorophenyl)]porphyrin Chloride Dissociation and the Creation of Catalytically Active Species for the Epoxidation of Cyclooctene

Ned A. Stephenson and Alexis T. Bell*

Chemical Sciences Division, Lawrence Berkeley Laboratory, and
Department of Chemical Engineering, University of California, Berkeley, California 94720-1462

Received December 8, 2005

In a previous study, the authors showed that iron(III) [tetrakis(pentafluorophenyl)]porphyrin chloride [(F₂₀TPP)FeCl] is catalytically inactive for cyclooctene epoxidation by hydrogen peroxide in acetonitrile but is catalytically active if the solvent contains methanol. It was suggested that the precursor to the active species is (F₂₀TPP)Fe(OCH₃) in methanol-containing solvents. The present study was aimed at evaluating this hypothesis. (F₂₀TPP)Fe(OCH₃) was synthesized and characterized by ¹H NMR but was found to be inactive in both acetonitrile and methanol. Further investigation of the interactions of (F₂₀TPP)FeCl with methanol in acetonitrile/methanol mixtures was then carried out using NMR. Two species, characterized by ¹H NMR resonances at 82 and 65 ppm, were observed. The first resonance is attributed to the β-pyrrole protons on molecularly dissolved (F₂₀TPP)FeCl, whereas the second is attributed to β-pyrrole protons of [(F₂₀TPP)Fe]⁺ cations that are stabilized by coordination with a molecule of methanol, viz., [(F₂₀TPP)Fe(CH₃OH)]⁺. The relative concentration of [(F₂₀TPP)Fe(CH₃OH)]⁺ increases as the fraction of methanol in the solvent increases, suggesting that methanol facilitates the dissociation of (F₂₀TPP)FeCl into cations and anions. A thermodynamic model of the dissociation is proposed and found to describe successfully the experimental observation over a range of solvent compositions, porphyrin concentrations, and temperatures. UV–visible spectroscopy was also used to validate the developed model. In addition, the observed rate constant for cyclooctene epoxidation was found to be proportional to the concentration of [(F₂₀TPP)Fe(CH₃OH)]⁺ calculated using the thermodynamic model, suggesting that this intermediate is a precursor to the species that catalyzes olefin epoxidation. The catalytic activity of [(F₂₀TPP)Fe(CH₃OH)]⁺ was further confirmed through experiments in which (F₂₀TPP)Fe(OCH₃) dissolved in methanol was reacted with HCl(aq). This reaction produced a product with an NMR peak at 65 ppm attributable to [(F₂₀TPP)Fe(CH₃OH)]⁺, and this mixture was found to have activity for cyclooctene epoxidation similar to that of (F₂₀TPP)FeCl dissolved in methanol.

Introduction

Iron(III) porphyrins are highly active catalysts for the oxidation of various organic substrates by either hydrogen peroxide or organic peroxides, and as a result, considerable attention has been devoted to understanding the effects of the porphyrin and solvent compositions on the mechanism and kinetics of such reactions.^{1–22} These studies have revealed that when the iron(III) porphyrin cation is charge-

compensated by a strongly bound ligand, such as Cl⁻, the porphyrin is totally inactive when dissolved in an aprotic solvent, such as acetonitrile, but becomes active in a mixture of protic and aprotic solvents.^{12–21} On the other hand, when

* To whom correspondence should be addressed. E-mail: bell@cchem.berkeley.edu.

(1) Sheldon, R. A. *Metalloporphyrins in Catalytic Oxidations*; Marcel Dekker: New York, 1994.

(2) Montanari, F.; Casella, L. *Metalloporphyrins Catalyzed Oxidations*; Kluwer Academic Publishers: Boston, 1994.

(3) Meunier, B. *Biomimetic Oxidations Catalyzed by Transition Metal Complexes*; Imperial College Press: London, 1999.

(4) Bruice, T. C. *Acc. Chem. Res.* **1991**, *24*, 243–249.

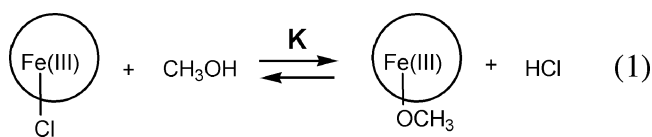
(5) Traylor, T. G.; Kim, C.; Fann, W. P.; Perrin, C. L. *Tetrahedron* **1998**, *54*, 7977–7986.

(6) Fujii, H. *Chem. Lett.* **1994**, 1491–1494.

(7) Almarsson, O.; Bruice, T. C. *J. Am. Chem. Soc.* **1995**, *117*, 4533–4544.

the iron(III) porphyrin is charge-compensated by a weakly bound anion, such as CF_3SO_3^- , the porphyrin is active even in aprotic solvents.^{20,21} While it is recognized that the catalytic activity of iron(III) porphyrins is affected by the composition of the axial ligand, the exact nature of the catalytically active form of the porphyrin is not well understood.^{17,19–22} Moreover, the relative strength of coordination of iron(III) porphyrin cations by different anions continues to be a subject of ongoing discussion.^{23–25}

In a recent investigation of the mechanism and kinetics of cyclooctene epoxidation by hydrogen peroxide catalyzed by iron(III) [tetrakis(pentafluorophenyl)]porphyrin chloride $[(\text{F}_{20}\text{TPP})\text{FeCl}]$, we observed that $(\text{F}_{20}\text{TPP})\text{FeCl}$ was inactive in acetonitrile but became active when a mixture of methanol and acetonitrile was used as the solvent.²⁶ On the basis of several observations, it was suggested that activation of the porphyrin complex involves the replacement of the chloride anion by a methoxide anion. In particular, the appearance of the latter species was suggested by the appearance of a new β -pyrrole proton NMR peak when $(\text{F}_{20}\text{TPP})\text{FeCl}$ was dissolved in a mixture of methanol and acetonitrile. Furthermore, a nonlinear relationship was observed between the rate constant and the total porphyrin concentration. This relationship was found to be consistent with a proposed equilibrium relationship between the chloride- and methoxide-coordinated forms of the porphyrin, as given by reaction 1.



The present investigation was undertaken to establish whether the methoxide-coordinated porphyrin cation, $(\text{F}_{20}$ -

$\text{TPP})\text{Fe}(\text{OCH}_3)$, or some other porphyrin species represents the precursor to the catalytically active form of $(\text{F}_{20}\text{TPP})\text{Fe}$. To this end, we synthesized $(\text{F}_{20}\text{TPP})\text{Fe}(\text{OCH}_3)$ and examined its ability to catalyze the epoxidation of cyclooctene by hydrogen peroxide. Because $(\text{F}_{20}\text{TPP})\text{Fe}(\text{OCH}_3)$ was found to be catalytically inactive, the nature of the active species formed upon dissolution of $(\text{F}_{20}\text{TPP})\text{FeCl}$ in a mixture of methanol and acetonitrile was investigated in more detail. The results of these studies led to the conclusion that the precursor to the active intermediate for epoxidation is likely to be methanol-coordinated $(\text{F}_{20}\text{TPP})\text{Fe}$ cations, viz., $[(\text{F}_{20}\text{TPP})\text{Fe}(\text{CH}_3\text{OH})]^+$. The thermodynamics of forming these cations is discussed in detail.

Experimental Section

Reagents. Non-UV-grade acetonitrile (99.99%), methanol (99.98%), hydrogen peroxide (30%), and ethylene glycol (98%) were obtained from EMD Chemicals. Iron(III) [tetrakis(pentafluorophenyl)]porphyrin chloride $[(\text{F}_{20}\text{TPP})\text{FeCl}]$, tetrabutylammonium chloride ($\geq 97\%$), and dodecane (99+%) were obtained from Sigma-Aldrich. *cis*-Cyclooctene (95%) was obtained from Alfa-Aesar. Deuterium oxide (99.9%) and deuterated chloroform (99.8%) were obtained from Cambridge Isotope Laboratories, Inc. Sodium methoxide (30% in methanol) was obtained from Fluka. Benzene (99.9%) was obtained from Fisher Scientific. All solvents were used as purchased without further purification.

Synthesis of Methoxide-Coordinated Porphyrin. Methoxide-coordinated iron(III) [tetrakis(pentafluorophenyl)]porphyrin was synthesized using a procedure analogous to that reported for the synthesis of methoxide-coordinated iron(III) tetraphenylporphyrin.²⁷ $(\text{F}_{20}\text{TPP})\text{FeCl}$ (100 mg) was dissolved in a 50-mL mixture of benzene and methanol (5:2 by volume) in a 250-mL round-bottomed flask. Sodium methoxide in methanol (0.67 mL of a 30% w/w solution) was added to this mixture, causing it to change from dark green to dark red. The solution was stirred at room temperature for 1 h and then reduced to a small volume under vacuum. The crystals that precipitated were then separated by filtration and washed with methanol (0 °C). The resulting crystals were dried at 44 °C under 0.72 bar of vacuum. The synthesis resulted in a 97% yield with a purity of approximately 98% based upon NMR spectroscopy.

NMR Characterization of Porphyrin Samples. Paramagnetic ^1H NMR spectra of the porphyrin species were obtained using a 400-MHz VMX spectrometer. A 90° pulse was used. The spectral width was increased to 140 ppm, and the spectra were centered at 60 ppm. Because of the high concentration of methanol protons in the sample, it was necessary to use a low gain. A line-broadening factor of 75 Hz was used to increase the signal-to-noise ratio. On the basis of the line-width at half-maximum, the relaxation constant for the paramagnetic porphyrin peaks was estimated to be a few milliseconds; therefore, the time delay between scans, D_1 , was set to 25 ms. D_1 was set to 4 s when studying the axial ligand proton peaks in the 0–10 ppm range. The number of data points was set to 4000. The number of scans required to obtain a suitable signal-to-noise ratio was dependent on the relative intensities of the two

- (8) He, G. X.; Bruce, T. C. *J. Am. Chem. Soc.* **1991**, *113*, 2747–2753.
 (9) Traylor, T. G.; Fann, W. P.; Bandyopadhyay, D. *J. Am. Chem. Soc.* **1989**, *111*, 8009–8010.
 (10) Traylor, T. G.; Xu, F. *J. Am. Chem. Soc.* **1987**, *109*, 6201–6202.
 (11) Nam, W.; Lim, M. H.; Moon, S. K.; Kim, C. *J. Am. Chem. Soc.* **2000**, *122*, 10805–10809.
 (12) Traylor, T. G.; Tsuchiya, S.; Byun, Y. S.; Kim, C. *J. Am. Chem. Soc.* **1993**, *115*, 2775–2781.
 (13) Traylor, T. G.; Kim, C.; Richards, J. L.; Xu, F.; Perrin, C. L. *J. Am. Chem. Soc.* **1995**, *117*, 3468–3474.
 (14) Nam, W.; Lim, M. H.; Lee, H. J.; Kim, C. *J. Am. Chem. Soc.* **2000**, *122*, 6641–6647.
 (15) Traylor, T. G.; Xu, F. *J. Am. Chem. Soc.* **1990**, *112*, 178–186.
 (16) Traylor, T. G.; Ciccone, J. P. *J. Am. Chem. Soc.* **1989**, *111*, 8413–8420.
 (17) Nam, W.; Lee, H. J.; Oh, S. Y.; Kim, C.; Jang, H. G. *J. Inorg. Biochem.* **2000**, *80*, 219–225.
 (18) Lee, K. A.; Nam, W. *J. Am. Chem. Soc.* **1997**, *119*, 1916–1922.
 (19) Nam, W.; Oh, S. Y.; Sun, Y. J.; Kim, J.; Kim, W. K.; Woo, S. K.; Shin, W. *J. Org. Chem.* **2003**, *68*, 7903–7906.
 (20) Nam, W.; Jin, S. W.; Lim, M. H.; Ryu, J. Y.; Kim, C. *Inorg. Chem.* **2002**, *41*, 3647–3652.
 (21) Nam, W.; Lim, M. H.; Oh, S. Y.; Lee, J. H.; Lee, H. J.; Woo, S. K.; Kim, C.; Shin, W. *Angew. Chem., Int. Ed.* **2000**, *39*, 3646–3649.
 (22) Goh, Y. M.; Nam, W. *Inorg. Chem.* **1999**, *38*, 914–920.
 (23) Hoshino, A.; Nakamura, M. *Chem. Lett.* **2004**, *33*, 1234–1235.
 (24) Song, B.; Park, B.; Han, C. *Bull. Korean Chem. Soc.* **2002**, *23*, 119–122.
 (25) Reed, C. A.; Guiset, F. *J. Am. Chem. Soc.* **1996**, *118*, 3281–3282.

- (26) Stephenson, N. A.; Bell, A. T. *J. Am. Chem. Soc.* **2005**, *127*, 8635–8643.
 (27) Otsuka, T.; Ohya, T.; Satu, M. *Inorg. Chem.* **1984**, *23*, 1777–1779.

peaks and ranged from 512 to 32 000. The total time to acquire a spectrum ranged from 1 min to 1 h.

Samples were prepared for NMR analysis by dissolving measured amounts of (F₂₀TPP)FeCl in 400 μ L of solvent in precision NMR tubes. A capillary filled with either D₂O or CDCl₃ was also placed in the NMR tube to serve as the locking solvent. For variable-temperature experiments, the temperature was monitored by a thermocouple located 2 mm from the tip of the sample tube and by an ethylene glycol-based NMR thermometer.²⁸ For the ethylene glycol thermometer, a second capillary with ethylene glycol was placed in the NMR tube; the presence of two capillaries required a reduction of the solvent volume to 300 μ L. To verify that the presence of two capillary tubes in the NMR tube does not affect the readings, separate measurements were also taken using an NMR tube filled only with ethylene glycol and a single capillary filled with the lock solvent; no difference in the temperature was observed between the two methods. Values from both the thermocouple and the NMR thermometer were always within 2 °C of each other; the NMR thermometer temperatures were used for all calculations. Several minutes were allowed for thermal equilibration at each temperature before acquiring a spectrum. In addition, duplicate spectra were taken to verify temperature stability; the difference between the two spectra was always negligible. Temperature stability was also tested by observing a constant-temperature reading from the NMR thermometer. Analysis of NMR spectra and peak integration was done in Origin 7.0.

UV–Visible Spectroscopy. Coordination of methanol to (F₂₀TPP)FeCl was studied by absorbance experiments using a Varian Cary 400 Bio UV–visible spectrometer. (F₂₀TPP)FeCl (25 μ M) was dissolved in acetonitrile, and methanol was then added in increments ranging from 5 to 50 μ L. A UV–visible spectrum was taken after each methanol addition. Reactions with hydrogen peroxide were also studied in situ by taking scans approximately every 1 min over the course of 20–30 min after the addition of hydrogen peroxide. Epoxidation reactions were studied by combining the catalyst (25 mM final concentration), the solvent (3.26 mL), cyclooctene (66 μ L), and hydrogen peroxide (1 μ L of a 30% w/w aqueous solution) in a 10-mm quartz spectrophotometer cell.

Cyclooctene Reactions. To investigate the epoxidation of cyclooctene, we combined the catalyst (75 μ M final concentration, unless stated otherwise), the solvent (3.0 mL), cyclooctene (330 μ L) and dodecane (10 μ L), as an internal standard, in a 5-mL glass vial with magnetic stirring. Hydrogen peroxide (5.0 μ L of a 30% w/w aqueous solution) was then added via a gastight syringe to initiate the reactions. At proper times, aliquots (0.5 μ L) from the reaction mixture were sampled and injected into an HP6890 series gas chromatograph fitted with an Agilent DB Wax (30 m \times 0.32 mm \times 0.5 μ m) capillary column and a flame ionization detector. The temperature program for analysis was as follows: 2.5 min at 50 °C, ramp at 20 °C/min to 175 °C, and 1.5 min at 175 °C. The split/splitless inlet was operated at 200 °C and 14.2 psi with a split ratio of 5. Dodecane and cyclooctene epoxide were eluted at 5.5 and 8.2 min, respectively. Data were obtained in triplicate to ensure precision, and the repeatability of the data was within \pm 2%. The accuracy of measuring the epoxide concentration via gas chromatography was determined to be \pm 1% by analysis of a calibrated standard. All chemicals were used as

packaged by the manufacturer without further purification or drying. Reactions were conducted under air because test reactions under nitrogen with deoxygenated solvents and substrate showed no difference. The presence of water was considered to be inconsequential. Solvents were not rigorously dried because the amount of water present in the added aqueous hydrogen peroxide solution is on the order of that present in the solvents. Furthermore, the addition of water in microliter aliquots was observed to not affect the kinetics.

Results and Discussion

Characterization of the Methoxide-Coordinated Species. The paramagnetic ¹H NMR spectrum of porphyrin produced by reaction of (F₂₀TPP)FeCl with sodium methoxide showed resonances at 81 and 4.9 ppm when dissolved in CDCl₃. The first of these features is very close to the position reported previously for β -pyrrole protons of porphyrins ligated by strongly bound axial ligands such as chloride, methoxide, and hydroxide anions,^{29–32} and the second feature is characteristic of protons associated with methoxy groups. The ratio of the peak areas for the peaks at 4.9 and 81 ppm is 0.38 and is very close to the 3:8 ratio expected for (F₂₀TPP)Fe(OCH₃). Both hydroxo and methoxide ligands are considered strong ligands as evidenced by ¹H NMR (β -pyrrole shifts near 80 ppm).^{29–32} If hydroxo-coordinated species were formed, they would readily convert to the μ -oxo species.³⁰ A small peak was observed at 14 ppm, suggesting the presence of μ -oxo species,²⁹ but this species accounts for less than 2% of the total porphyrin species. Therefore, the hydroxo-coordinated species very likely are not formed to any appreciable extent. Thus, on the basis of NMR analysis, we conclude that virtually pure (F₂₀TPP)Fe(OCH₃) was prepared.

Reactivity of the Methoxide-Coordinated Species. The activity of the (F₂₀TPP)Fe(OCH₃)-catalyzed cyclooctene epoxidation was investigated using hydrogen peroxide as the oxidant and methanol as the solvent. Upon dissolution of (F₂₀TPP)Fe(OCH₃), the solution turned dark orange. However, no epoxidation occurred over the course of several hours. The reaction mixture was analyzed via ¹H NMR spectroscopy after a period of 3.5 h. As evidenced by a ¹H NMR peak at 10.3 ppm,³³ hydrogen peroxide still remained in the solution. In situ UV–visible spectra of the reaction mixture showed a monotonic decrease in the intensity of the entire spectrum but no change in the peak shape as a function of time after hydrogen peroxide was added to the reaction mixture. As evidenced by complete bleaching of the por-

(28) Amman, C.; Meier, P.; Merbach, A. E. *J. Magn. Reson.* **1982**, *46*, 319–321.

(29) Birnbaum, E. R.; Hodge, J. A.; Grinstaff, M. W.; Schaefer, W. P.; Henling, L.; Labinger, J. A.; Bercaw, J. E.; Gray, H. B. *Inorg. Chem.* **1995**, *34*, 3625–3632.

(30) Cheng, R. J.; Latos-Grazynski, L.; Balch, A. L. *Inorg. Chem.* **1982**, *21*, 2412–2418.

(31) Woon, T. C.; Shirazi, A.; Bruce, T. C. *Inorg. Chem.* **1986**, *25*, 3845–3846.

(32) Groves, J. T.; Quinn, R.; McMurry, T. J.; Nakamura, M.; Lang, G.; Boso, B. *J. Am. Chem. Soc.* **1985**, *107*, 354–360.

(33) Stephenson, N. A.; Bell, A. T. *Anal. Bioanal. Chem.* **2005**, *381*, 1289–1293.

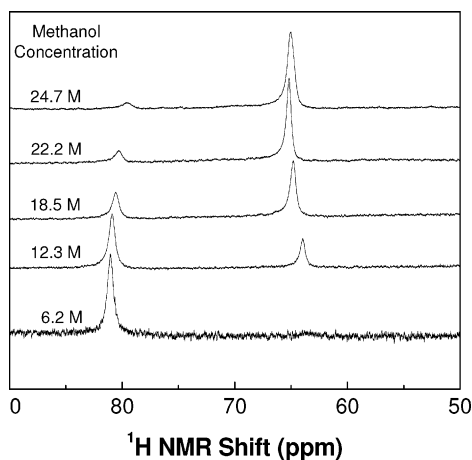


Figure 1. ^1H NMR spectra of $(\text{F}_{20}\text{TPP})\text{FeCl}$ dissolved in methanol/acetonitrile solutions. The total porphyrin concentration for each spectrum was ~ 15 mM.

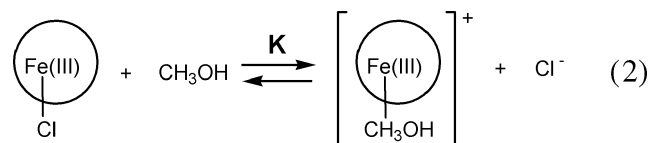
phyrin, the reactions ended because of complete destruction of the porphyrin and not because of complete consumption of the oxidant.

The inability of $(\text{F}_{20}\text{TPP})\text{Fe}(\text{OCH}_3)$ to catalyze the epoxidation of cyclooctene suggests that iron(IV) π -radical cation porphyrin species, the proposed active intermediates for epoxidation,²⁶ are not formed and, hence, that heterolytic cleavage of the oxygen–oxygen bond in the iron(III) hydroperoxide species does not occur when hydrogen peroxide interacts with $(\text{F}_{20}\text{TPP})\text{Fe}(\text{OCH}_3)$. Evidence was also not seen for homolytic cleavage of iron(III) hydroperoxide species because the occurrence of this process would have produced iron(IV) oxo species, which would have turned the solution bright red and resulted in a peak near 540 nm in the UV–visible spectrum of the solution.³⁴ Similar to the reaction of hydrogen peroxide with the chloride-coordinated species in aprotic solvents, only a small portion of the hydrogen peroxide was consumed over the course of several hours, with the only consequence being porphyrin degradation. The absence of either hydrogen peroxide decomposition or cyclooctene epoxidation indicates that some species other than $(\text{F}_{20}\text{TPP})\text{Fe}(\text{OCH}_3)$ must be the precursor to the intermediate responsible for olefin epoxidation when the chloride-coordinated porphyrin is dissolved in methanol.

Identification of the Precursor to the Active Intermediate. When $(\text{F}_{20}\text{TPP})\text{FeCl}$ is dissolved in acetonitrile, a dark-brown solution is obtained; the solution turns emerald green as methanol is substituted for the aprotic solvent. ^1H NMR spectra of these solutions for different concentrations of methanol are shown in Figure 1. In pure acetonitrile, a single peak is observed at 82 ppm, and as the mole fraction of methanol in the solvent increases, a new peak appears at 65 ppm and grows in intensity. At the same time, the peak at 82 ppm decreases in intensity. However, even in pure methanol (24.7 M), a small peak is still observed near 82 ppm. The observation of the peak near 82 ppm in both pure

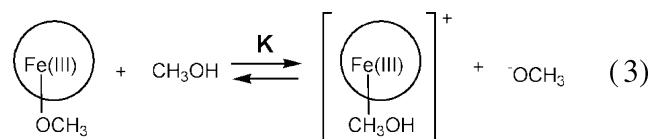
acetonitrile and pure methanol suggests that the species responsible for this peak are the same in both solvents and are not affected significantly by the solvent composition. Assignment of this peak to molecularly dissolved $(\text{F}_{20}\text{TPP})\text{FeCl}$ is fully consistent with previous studies, which show a β -pyrrole ^1H NMR peak near 80 ppm for iron tetraphenylporphyrins with tightly bound axial ligands.^{29–32} The exact position of the peak depends on the composition of the solvent, but this effect is limited to less than 5 ppm. The peak near 82 ppm shifts upfield while the peak near 65 ppm shifts slightly downfield as the methanol concentration is increased.

As the strength of the interaction of the ligand with the porphyrin decreases, the position of the β -pyrrole peak shifts upfield progressively from 80 ppm to as far as -62 ppm.^{23,25,32} We propose that the peak at 65 ppm is attributable to $[(\text{F}_{20}\text{TPP})\text{Fe}]^+$ cations, each of which is weakly coordinated to a molecule of methanol, i.e., $[(\text{F}_{20}\text{TPP})\text{Fe}(\text{CH}_3\text{OH})]^+$. The formation of such species requires the dissociation of $(\text{F}_{20}\text{TPP})\text{FeCl}$ into cations and anions. The endothermicity of this process is offset by the energy released via the coordination of methanol to the $[(\text{F}_{20}\text{TPP})\text{Fe}]^+$ cation and by the solvation of both the resulting $[(\text{F}_{20}\text{TPP})\text{Fe}(\text{CH}_3\text{OH})]^+$ cation and the Cl^- anion. Therefore, in the presence of methanol, $(\text{F}_{20}\text{TPP})\text{FeCl}$ is thought to dissociate via reaction 2.



The position of the β -pyrrole ^1H NMR peak at 65 ppm is consistent with the proposed attribution of this peak to $[(\text{F}_{20}\text{TPP})\text{Fe}(\text{CH}_3\text{OH})]^+$ rather than to $[(\text{F}_{20}\text{TPP})\text{Fe}]^+$. As noted above the interaction of $[(\text{F}_{20}\text{TPP})\text{Fe}]^+$ cations with very weakly bound ligands shifts the position of the β -pyrrole peak to -62 ppm.²⁵ The observation of a new peak at 65 ppm is characteristic of a weakly bound ligand similar to a triflate anion, which shows a β -pyrrole resonance at 57 ppm. This leads to the suggestion that methanol coordinated to $[(\text{F}_{20}\text{TPP})\text{Fe}]^+$ cations affects the shielding of the β -pyrrole hydrogen atoms on the porphyrin ring in much the same manner as a weakly bound anionic ligand.

An interesting question is why $(\text{F}_{20}\text{TPP})\text{Fe}(\text{OCH}_3)$ does not dissociate in a manner similar to that of $(\text{F}_{20}\text{TPP})\text{FeCl}$ when dissolved in methanol, viz., reaction 3. We attribute this to the fact that methoxide is a much stronger base than chloride. As a result, the methoxide anions would deprotonate any $[(\text{F}_{20}\text{TPP})\text{Fe}(\text{CH}_3\text{OH})]^+$ cations present in solution; therefore, reaction 3 does not occur.



(34) Lee, K. A.; Nam, W. *Bull. Korean Chem. Soc.* **1996**, *17*, 669–671.

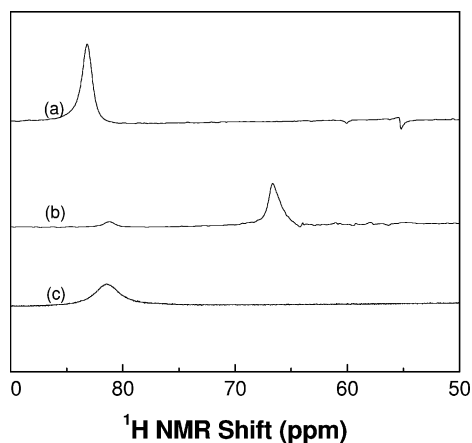


Figure 2. 1H NMR spectra of the methoxide-ligated porphyrin: (a) in acetonitrile with HCl; (b) in methanol with HCl; (c) in methanol without HCl. $[(F_{20}TPP)Fe(OCH_3)] \sim 11$ mM and $[HCl] \sim 25$ mM.

To test the arguments given above, we introduced free protons in the form of hydrochloric acid to a methanol solution of $(F_{20}TPP)Fe(OCH_3)$. A total of 2–3 equiv of HCl(aq) were added per 1 equiv of porphyrin. The solution immediately changed from dark orange to emerald green, and $[(F_{20}TPP)Fe(CH_3OH)]^+$ cations were formed, as evidenced by a decrease in the intensity of the β -pyrrole peak near 80 ppm and the formation of a β -pyrrole peak at 67 ppm (see Figure 2). Furthermore, as discussed below, the species created by the addition of hydrochloric acid to $(F_{20}TPP)Fe(OCH_3)$ in methanol exhibited similar catalytic activity for cyclooctene epoxidation as $(F_{20}TPP)FeCl$ dissolved in pure methanol, providing further support for the conclusion that dissociation of the porphyrin salt into $[(F_{20}TPP)Fe(CH_3OH)]^+$ and Cl^- is a necessary condition for catalysis to occur. As evidenced by no change in the position of the β -pyrrole resonance, formation of $[(F_{20}TPP)Fe(CH_3OH)]^+$ or any other weakly coordinated cationic porphyrin species was not evidenced when HCl(aq) was added to $(F_{20}TPP)Fe(OCH_3)$ dissolved in acetonitrile. We suggest that this is further evidence that acetonitrile is not capable of stabilizing the ionic products of reaction 2.

Thermodynamics of $(F_{20}TPP)FeCl$ Dissociation. An equilibrium relationship (eq 1) can be written between the species shown in reaction 2. Conservation of charge requires that the concentrations of both species on the right side of the equilibrated reaction be the same. Therefore, eq 1 can be rewritten as eq 2. If we also assume that the only porphyrin species are the chloride-coordinated species and the methanol-coordinated porphyrin cations, then a balance of porphyrin species results in eq 3, where $[Fe-Cl]_0$ is the concentration of all porphyrin species in solution. Combining eqs 2 and 3 leads to a quadratic relationship between the concentration of the methanol-coordinated porphyrin cations and the methanol concentration (eq 4). This relationship also predicts that the concentration of methanol-coordinated porphyrin cations will be a nonlinear function of the total porphyrin concentration, $[Fe-Cl]_0$.

$$K = \frac{[Fe-CH_3OH^+][Cl^-]}{[Fe-Cl][CH_3OH]} \quad (1)$$

$$K = \frac{[Fe-CH_3OH^+]^2}{[Fe-Cl][CH_3OH]} \quad (2)$$

$$[Fe-Cl]_0 = [Fe-CH_3OH^+] + [Fe-Cl] \quad (3)$$

$$[Fe-CH_3OH^+] = \left\{ -K[CH_3OH] + \sqrt{(K[CH_3OH])^2 + 4K[CH_3OH][Fe-Cl]_0} \right\} / 2 \quad (4)$$

Several experiments were designed to test the validity of our proposed model. In a previous publication, we had used eq 4 to determine the value of K by varying the total porphyrin concentration.²⁶ In that experiment, we discovered that the observed rate constant for the epoxidation of cyclooctene did not increase linearly with the total porphyrin concentration. Using eq 4 to calculate $[(F_{20}TPP)Fe(CH_3OH)]^+$, we were able to show that the observed rate constant increases linearly with $[(F_{20}TPP)Fe(CH_3OH)]^+$. (Note: the previous publication refers to this species as the methoxide-ligated porphyrin species.) A value of $K = 1.2 \times 10^{-5}$ was obtained in that study.²⁶

If the species responsible for the NMR peak at 65 ppm are due to methanol-coordinated porphyrin cations, the species responsible for the peak at 82 ppm are due to chloride-coordinated species, and the equilibrium relationship given by eq 1 is correct, then the equilibrium constant determined from an analysis of the paramagnetic NMR data should agree with the value previously obtained by analysis of the reaction kinetics. The equilibrium constant K was determined by fitting eq 4 to the NMR data obtained in an experiment in which the total porphyrin concentration was varied, and the results are shown in Figure 3. $[Fe-Cl]$ was determined from the area of the peak at 82 ppm, and $[Fe-CH_3OH^+]$ was determined from the area of the peak at 65 ppm. The value of K obtained in this way is 1.0×10^{-5} , which is in excellent agreement with the value previously obtained from kinetics.²⁶ It is also notable that the concentrations of porphyrin used for each of the two sets of experiments are noticeably different. The total porphyrin concentration used for the measurements of epoxidation kinetics ranged from $37 \mu M$ to 0.9 mM, whereas the NMR experiments reported here were carried out using a total porphyrin concentration ranging from 1.8 to 15 mM. Therefore, as shown by two methods, eq 4 fits the observed data over a wide range of porphyrin concentrations for a given methanol concentration.

To validate the model further, eq 4 was used to fit the equilibrium constant to NMR data taken at different methanol concentrations. Data fits similar to the one shown in Figure 3 were obtained in each case. Figure 4 shows that the equilibrium constant increases exponentially with the methanol concentration, resulting in a sigmoidal relationship between the concentration of the methanol-coordinated species and the methanol concentration (see Figure 5).

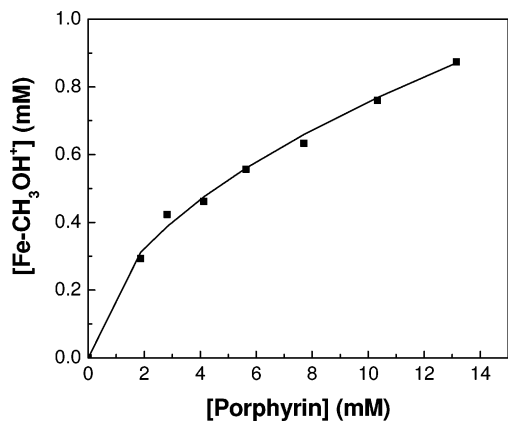


Figure 3. Plot of the concentration of $[(F_{20}TPP)Fe(CH_3OH)]^+$ vs the total porphyrin concentration. The solid curve represents a fit of eq 4 to the data for a value of $K = 1.0 \times 10^{-5}$ when the methanol concentration is 6.175 M.

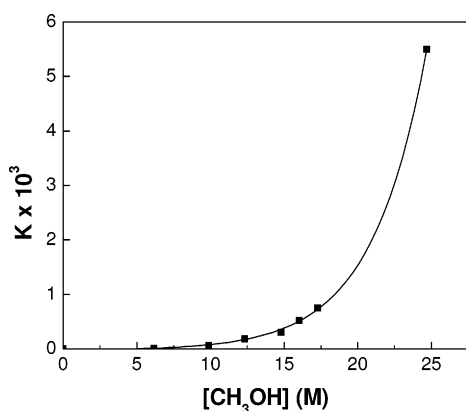


Figure 4. Plot of the equilibrium constant determined experimentally vs the methanol concentration.

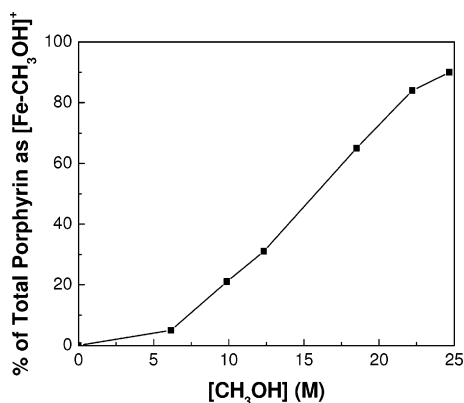


Figure 5. Plot of the concentration of $[(F_{20}TPP)Fe(CH_3OH)]^+$ vs the concentration of methanol in the solvent. Data are shown for a porphyrin concentration of ~ 15 mM.

Because the equilibrium constant can be expressed in terms of the Gibbs free energy (eq 5), we hypothesized that the enthalpy change is linearly proportional to the methanol concentration, as shown in eq 6. Upon substitution and rearrangement, eq 5 can be rewritten as eq 7, where K_0 is equal to $e^{\Delta S^\circ/R}$. This equation can be simplified to eq 8, where K_1 is equal to $K_0 e^{-\Delta H_0^\circ/RT}$. As shown in Figure 6, the value of α , as determined from the slope of a plot of $\ln(K)$ vs

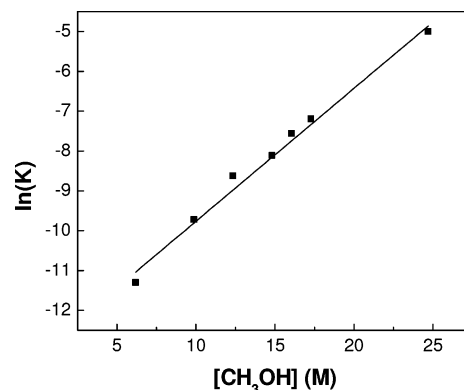


Figure 6. Plot of $\ln(K)$ vs $[CH_3OH]$. All data are for room temperature at ~ 23 °C.

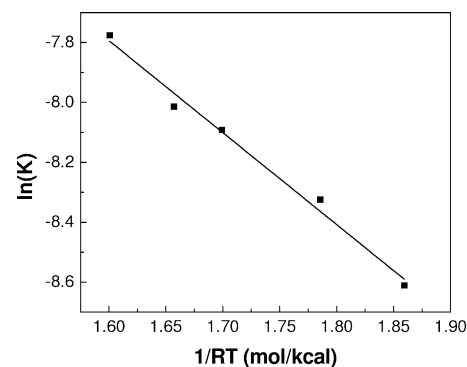


Figure 7. Plot of $\ln(K)$ vs $1/RT$. All data are for a methanol concentration of 14.8 M.

methanol concentration, is found to be -0.20 kcal \cdot L/mol 2 .

$$K = e^{-\Delta G^\circ/RT} \quad (5)$$

$$\Delta H^\circ = \Delta H_0^\circ + \alpha[CH_3OH] \quad (6)$$

$$K = K_0 e^{-\Delta H^\circ/RT} \quad (7)$$

$$K = K_1 e^{-\alpha[CH_3OH]/RT} \quad (8)$$

Additional NMR experiments were conducted at a fixed methanol concentration while varying the temperature between 0 and 40 °C. A methanol concentration of 14.8 M was chosen for these experiments. This choice of conditions resulted in the peaks at 65 and 82 ppm having roughly equal areas, allowing the number of scans required for a reasonable signal-to-noise ratio to be a minimum. As expected for paramagnetic species, the peak positions of both species showed Curie-type behavior, shifting linearly with the inverse of temperature. The observed equilibrium constant was determined for each temperature and plotted as a function of $1/RT$, as seen in Figure 7. Fitting of the data shown in Figures 6 and 7 results in $\Delta H_0^\circ = 6.0 \pm 0.3$ kcal/mol, $\alpha = -0.20 \pm 0.01$ kcal \cdot L/mol 2 , and $\Delta S^\circ = -5.8 \pm 0.6$ cal/mol \cdot K, where the equilibrium constant is expressed according to eq 9.

$$K = e^{-(\Delta H_0^\circ + \alpha[CH_3OH])/RT} e^{\Delta S^\circ/R} \quad (9)$$

To show that the experimentally determined thermodynamic parameters are valid over a wide range of data, two additional analyses were conducted. The variable-temperature experiment was repeated using a sample with a methanol concentration of 9.9 M; analysis of the plot of $\ln(K)$ vs $1/RT$, not shown, gives $\alpha = -0.20$ kcal·L/mol² and $\Delta S = -5.8$ cal/mol·K, values that are identical with those obtained for a methanol concentration of 14.8 M. In addition, the value of ΔS° was determined by using the equilibrium constants determined at room temperature for methanol concentrations between 6.2 and 24.7 M. ΔG° was calculated as a function of the methanol concentration using eq 5. ΔS° was then determined by subtracting ΔH° , as calculated from eq 6, from ΔG° and dividing by the temperature. ΔS° determined in this way is equal to -5.9 ± 0.8 cal/mol·K and is independent of the methanol concentration.

On the basis of the above analysis, the value of ΔH_0° is positive, indicating that the dissociation of (F₂₀TPP)FeCl is endothermic. This indicates that the enthalpies of solvation of the cations and anions formed upon dissociation of this porphyrin are not sufficiently negative to offset the positive enthalpy required to form the cation and anion pair. The value of α is negative as well, indicating that the value of ΔH° decreases with an increase in the methanol fraction in the solvent mixture. As discussed above, the decrease in ΔH° with an increase in the methanol content of the solvent is due to increased solvation of the chloride anions, as well as to stabilization of the [(F₂₀TPP)Fe]⁺ cations through coordination with methanol. Nevertheless, ΔH° remains positive even in pure methanol. It is also found that ΔS° is negative, which indicates an increase in order when (F₂₀TPP)FeCl dissociates. Because the number of species before and after dissociation (see reaction 2) does not change, the negative sign is likely due to an increase in the solvent ordering around the cations and anions formed upon dissociation of (F₂₀TPP)FeCl, relative to the undissociated porphyrin.

As a further test of the validity of the thermodynamic model described above for reaction 2, an experiment was carried out in which chloride anions were added to the mixture using tetrabutylammonium chloride as the source. The experiment was conducted in a solvent mixture containing equal volume amounts of methanol and acetonitrile; chloride anions, 0.72 equiv relative to the concentration of the porphyrin species, were added to the solution. Consistent with the model for reaction 2, the addition of chloride anions shifted the equilibrium to the left. This particular salt was used because the tetrabutylammonium cation was not expected to affect reaction 2. Prior to chloride addition, approximately 30% of the porphyrin species was coordinated to methanol, while only 13% was methanol-coordinated after the addition of the chloride source. The model for the equilibrium constant presented above predicts that 12.5% of the porphyrin species should be coordinated to methanol after the addition of 0.72 equiv of chloride.

Application of the Model to Lower Porphyrin Concentrations. In efforts to minimize the instrument time

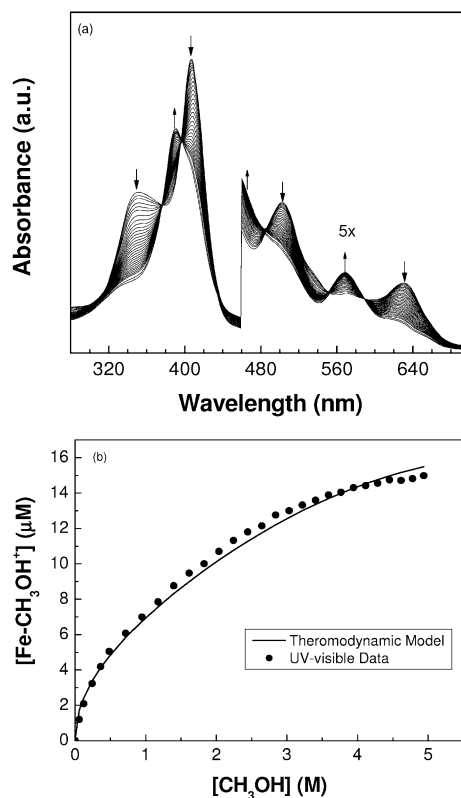


Figure 8. (a) UV-visible spectra obtained by methanol addition to (F₂₀TPP)FeCl dissolved in acetonitrile. Arrows indicate the direction of the absorbance change with an increase in the methanol concentration. (b) Comparison of the concentration of [(F₂₀TPP)Fe(CH₃OH)]⁺ as determined from the spectra in part a to the thermodynamic model. The initial total porphyrin concentration was 25 μ M.

required to obtain data, NMR spectroscopy experiments were conducted using much higher porphyrin concentrations relative to the concentration used for kinetic studies (10 mM vs 75 μ M). Additional experiments using UV-visible spectroscopy were conducted to show that the thermodynamic model presented above is applicable at lower porphyrin concentrations. Because of absorbance limitations, a porphyrin concentration of 25 μ M was used for these experiments. (F₂₀TPP)FeCl was dissolved in acetonitrile, and microliter quantities of methanol were added incrementally to the solution. The resulting spectra are shown in Figure 8a; note that the systematic decrease in the absorbance is due to dilution of the porphyrin concentration as a result of methanol addition. Addition of methanol results in a decrease in the absorbance of the Soret peak at 407 nm and the formation and subsequent increase of a new Soret peak at 390 nm; new features are also formed at 460 and 569 nm (see Figure 8a). Clear isosbestic points are seen at 376, 396, 484, 551, and 589 nm. We attribute these changes in the UV-visible spectra to an exchange of the chloride ligand for a methanol solvent molecule. The change in absorbance at 569 nm was used to determine the concentration of [(F₂₀TPP)Fe(CH₃OH)]⁺ as a function of the methanol concentration; this peak was chosen because it was the best resolved of the newly formed peaks. As shown in Figure 8b, the change in the concentration of [(F₂₀TPP)Fe(CH₃OH)]⁺ with

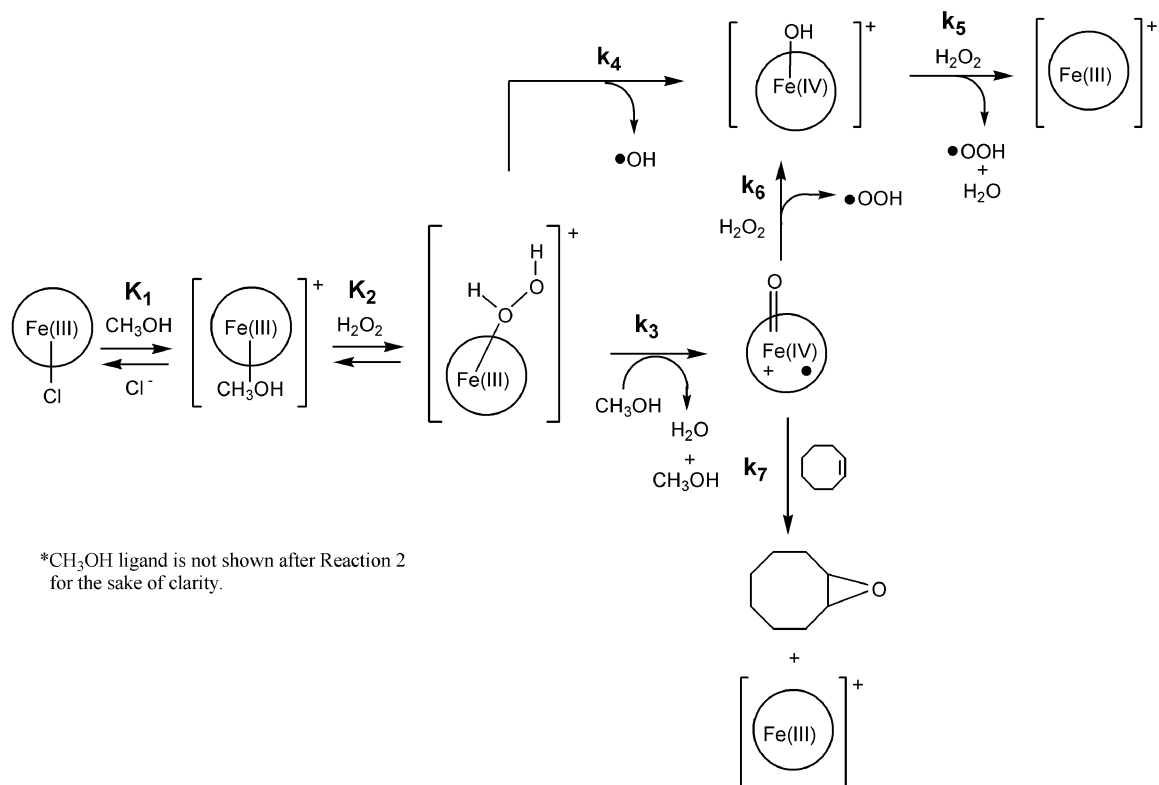


Figure 9. Proposed mechanism for (F₂₀TPP)FeCl-catalyzed epoxidation of cyclooctene using hydrogen peroxide as the oxidant.

the methanol concentration determined from the UV–visible spectra is in excellent agreement with that predicted by the thermodynamic model. Therefore, the model developed via NMR spectroscopy at high porphyrin concentrations is valid for porphyrin concentrations over 3 orders of magnitude (10 μ M to 10 mM).

Implications for the Kinetics of Cyclooctene Epoxidation. As noted in the Introduction, we have previously investigated the kinetics of cyclooctene epoxidation by H₂O₂ catalyzed by (F₂₀TPP)FeCl dissolved in mixtures of acetonitrile and methanol.^{26,35} The kinetics of this reaction are well described over a wide range of conditions by rate expressions derived from the mechanism shown in Figure 9.^{26,35} In reaction 1, (F₂₀TPP)FeCl dissociates to form [(F₂₀TPP)Fe(CH₃OH)]⁺ and Cl⁻. The first of these species then coordinates H₂O₂ reversibly in reaction 2. The heterolytic and homolytic cleavages of the O–O bond of H₂O₂ occur in reactions 3 and 4, the first of which involves the direct participation of methanol. The iron(IV) π -radical cation formed via reaction 3 can then react with cyclooctene to produce cyclooctene epoxide (reaction 7) or with H₂O₂ to produce free radicals and the products of peroxide decomposition (reactions 6 and 5). When the concentration of cyclooctene to H₂O₂ is in excess, the rate of reaction 7 greatly exceeds that of reaction 6. Under these conditions, the rate coefficient (k_{obs}) for the consumption of H₂O₂, the limiting reagent, is given by eq 10.^{26,35} [Fe–CH₃OH⁺] is the concentration of methanol-coordinated porphyrin

cations, and Y_{∞} is the yield of epoxide determined at the point of complete consumption of H₂O₂, as defined by eq 11. The yield is used to relate the rate of epoxide formation to the overall rate of hydrogen peroxide consumption.

$$k_{\text{obs}} = \frac{k_3 K_2 [\text{Fe}-\text{CH}_3\text{OH}^+][\text{CH}_3\text{OH}]}{Y_{\infty}} \quad (10)$$

$$Y_{\infty} = \frac{[\text{C}_8\text{-O}]_{\infty}}{[\text{H}_2\text{O}_2]_0} \times 100\% \cong \frac{k_3 [\text{CH}_3\text{OH}]}{k_3 [\text{CH}_3\text{OH}] + 2k_4} \times 100\% \quad (11)$$

In our initial studies of cyclooctene epoxidation by H₂O₂ catalyzed by (F₂₀TPP)FeCl dissolved in methanol/acetonitrile mixtures, the value of k_{obs} was found to increase nonlinearly with the concentration of (F₂₀TPP)FeCl for a fixed solvent composition.²⁶ The question to be addressed is whether k_{obs} is linearly proportional to the concentration of [(F₂₀TPP)Fe(CH₃OH)]⁺, as indicated by eq 10. Figure 10a shows that k_{obs} indeed increases linearly with the concentration of [(F₂₀TPP)Fe(CH₃OH)]⁺, as determined from eq 4. When the concentration of (F₂₀TPP)FeCl is held constant but the concentration of methanol is varied, k_{obs} is predicted to increase linearly with the ratio of [Fe–CH₃OH⁺][CH₃OH] to Y_{∞} . Figure 10b shows such a plot and further demonstrates the agreement between theory and experiment. Therefore, the equilibrium relationship based on reaction 2 is fully consistent, not only with the NMR and UV–visible observations but also with the kinetics for the epoxidation of cyclooctene.^{26,35}

(35) Stephenson, N. A.; Bell, A. T. *Inorg. Chem.* **2006**, in press.

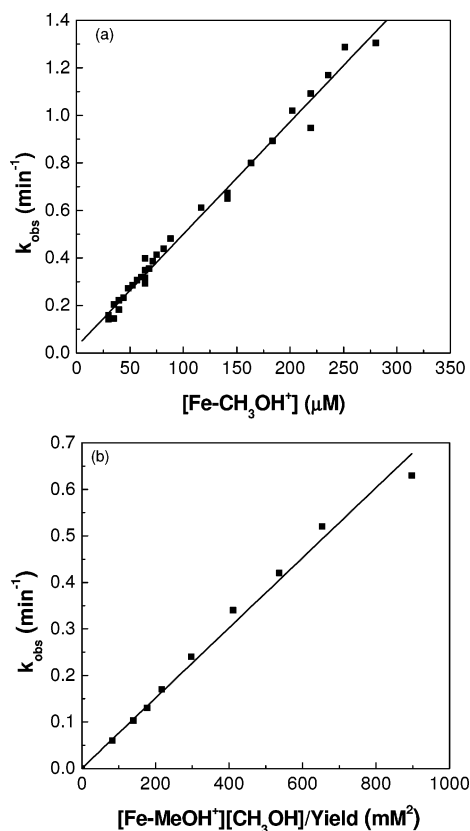


Figure 10. (a) Plot of k_{obs} vs the concentration of $[(F_{20}\text{TPP})\text{Fe}(\text{CH}_3\text{OH})]^+$ for experiments with a constant concentration of CH_3OH (~ 6.3 M) and varying concentrations of $(F_{20}\text{TPP})\text{FeCl}$. (b) Plot of k_{obs} vs the concentration of $[(F_{20}\text{TPP})\text{Fe}(\text{CH}_3\text{OH})]^+$ times the concentration of CH_3OH divided by the yield of cyclooctene epoxide. In this case, the concentration of $[(F_{20}\text{TPP})\text{Fe}(\text{CH}_3\text{OH})]^+$ was varied by changing the concentration of CH_3OH while holding the concentration of $(F_{20}\text{TPP})\text{FeCl}$ constant at ~ 75 μM .

Because the reaction of $(F_{20}\text{TPP})\text{Fe}(\text{OCH}_3)$ with $\text{HCl}(\text{aq})$ in methanol produces $[(F_{20}\text{TPP})\text{Fe}(\text{CH}_3\text{OH})]^+$, an experiment was carried out to determine whether $[(F_{20}\text{TPP})\text{Fe}(\text{CH}_3\text{OH})]^+$ produced in this way would catalyze the epoxidation of cyclooctene. For this experiment, 40 equiv of $\text{HCl}(\text{aq})$ was added per 1 equiv of $(F_{20}\text{TPP})\text{Fe}(\text{OCH}_3)$ dissolved in methanol. A value for k_{obs} of 0.4 min^{-1} was obtained, which is similar to that obtained when $(F_{20}\text{TPP})\text{FeCl}$ is dissolved in methanol, 0.6 min^{-1} . The yield of cyclooctene epoxide was also virtually the same in both cases, 88%. These results

further support the hypothesis that $[(F_{20}\text{TPP})\text{Fe}(\text{CH}_3\text{OH})]^+$ is a critical intermediate in the epoxidation of olefins by hydrogen peroxide in methanol-containing solutions of $(F_{20}\text{TPP})\text{FeCl}$.

Conclusions

We have shown that $(F_{20}\text{TPP})\text{FeCl}$ is dissolved molecularly in acetonitrile but dissociatively in mixtures of acetonitrile and methanol. In the latter case, the iron(III) porphyrin cation is stabilized by a molecule of methanol as $[(F_{20}\text{TPP})\text{Fe}(\text{CH}_3\text{OH})]^+$. A similar cation is not formed, though, when $(F_{20}\text{TPP})\text{Fe}(\text{OCH}_3)$ is dissolved in pure methanol. The lower degree of dissociation for $(F_{20}\text{TPP})\text{Fe}(\text{OCH}_3)$ relative to $(F_{20}\text{TPP})\text{FeCl}$ in methanol is due to the much higher basicity of methoxide anions relative to chloride anions. However, $[(F_{20}\text{TPP})\text{Fe}(\text{CH}_3\text{OH})]^+$ cations can be formed from $(F_{20}\text{TPP})\text{Fe}(\text{OCH}_3)$ dissolved in methanol when $\text{HCl}(\text{aq})$ is added to the solution. The thermodynamic parameters that determine the equilibrium constant for the dissociation of $(F_{20}\text{TPP})\text{FeCl}$ in methanol-containing solutions, ΔH° and ΔS° , have been evaluated, and the proposed model for $(F_{20}\text{TPP})\text{FeCl}$ dissociation has been shown to be valid over a range of temperatures, methanol concentrations, and porphyrin concentrations. We have also shown that $[(F_{20}\text{TPP})\text{Fe}(\text{CH}_3\text{OH})]^+$ cations formed via dissociation of $(F_{20}\text{TPP})\text{FeCl}$ in methanol-containing solutions are necessary intermediates in the epoxidation of cyclooctene by H_2O_2 . Furthermore, we have shown that the observed rate constant for the consumption of H_2O_2 , k_{obs} , is linearly proportional to the concentration of $[(F_{20}\text{TPP})\text{Fe}(\text{CH}_3\text{OH})]^+$.

Acknowledgment. The authors thank Rudi Nunlist for his help in optimizing the parameters used for the paramagnetic NMR experiments and John Prausnitz and John Newman for their helpful discussions concerning the thermodynamics of porphyrin dissociation. The authors also thank the reviewers of this work for their constructive comments and suggestions, which have led to an improvement in the presentation of our work. This work was supported by the Director, Office of Basic Energy Sciences, Chemical Sciences Division of the U.S. Department of Energy under Contract DE-AC02-05CH11231.

IC0521067